where $H_n = S_n - (\bar{X} - \mu)(\bar{X} - \mu)^{\mathrm{T}}$. Thus, $q_n(\mu)$ can be readily computed without solving the nonlinear equation (5) as for the full empirical likelihood. The least-squares empirical likelihood ratio is a first-order approximation to the full empirical likelihood ratio, and $q_n(\mu) \to \chi_p^2$ in distribution when p is fixed.

The least-squares empirical likelihood is less affected by higher dimension. In particular, if $k \geqslant 3$ in (4), then

$$(2p)^{-1/2}\{q_n(\mu) - p\} \to N(0, 1) \tag{12}$$

in distribution as $n \to \infty$ when $p = o(n^{2/3})$, which improves the rate given by Theorem 3 for the full empirical likelihood ratio $w_n(\mu)$.

To appreciate (12), we note from (11) that

$$q_n(\mu) = n(\bar{X} - \mu)^{\mathrm{T}}\Sigma^{-1}(\bar{X} - \mu) + n(\bar{X} - \mu)^{\mathrm{T}}(H_n^{-1} - \Sigma^{-1})(\bar{X} - \mu). \tag{13}$$

Then, following a similar line to the proof of Lemma 6,

$$n(\bar{X} - \mu)^{\mathrm{T}}(H_n^{-1} - \Sigma^{-1})(\bar{X} - \mu) = O_p(p^2/n) = o_p(p^{1/2}).$$

As the first term on the right-hand side of (13) is asymptotically normal with mean p and variance $2p$ as conveyed in (10), (12) is valid.

If we confine ourselves to specific distributions, faster rates for p can be established. For example, if the data are normally distributed, the least-squares empirical likelihood ratio is the Hotelling-T^2 statistic, which is shown in Bai & Saranadasa (1996) to be asymptotically normal if $p/n \to c \in [0, 1)$.

4. NUMERICAL RESULTS

We report results from a simulation study designed to evaluate the asymptotic normality of the empirical likelihood ratio. The $p \times 1$ independent and identically distributed data vectors $\{X_i\}_{i=1}^n$ were generated from a moving average model,

$$X_{ij} = Z_{ij} + \rho Z_{ij+1} \quad (i = 1, \ldots, n, \quad j = 1, \ldots, p),$$

where, for each i, the innovations $\{Z_{ij}\}_{j=1}^{p+1}$ were independent random variables with zero mean and unit variance. We considered two distributions for the innovation Z_{ij}. One is the standard normal distribution, and the other is a standardized version of a Pareto distribution with distribution function $(1 - x^{-4\cdot5})I(x \geqslant 1)$. We standardized the Pareto random variables so that they had zero mean and unit variance. As the Pareto distribution has only four finite moments, we had $k = 1$ in (4), whereas $k = \infty$ for the normally distributed innovations. In both distributions, X_i is a multivariate random vector with zero mean and covariance $\Sigma = (\sigma_{ij})_{p\times p}$, where $\sigma_{ii} = 1$, $\sigma_{ii\pm1} = \rho$ and $\sigma_{ij} = 0$ for $|i - j| > 1$. We set ρ to be 0·5 throughout the simulation.

To make p and n increase simultaneously, we considered two growth rates for p with respect to n: (i) $p = c_1 n^{0\cdot4}$ and (ii) $p = c_2 n^{0\cdot24}$. We chose the sample size $n = 200$, 400 and 800. By assigning $c_1 = 3$, 4 and 5 in the faster growth rate setting (i), we obtained three dimensions for each sample size, which were $p = 25$, 33 and 43 for $n = 200$; $p = 33$, 44 and 58 for $n = 400$; and $p = 42$, 55 and 72 for $n = 800$, respectively. For the slower growth rate setting (ii), to maintain a certain amount of increase between successive dimensions when n was increased, we assigned larger $c_2 = 4$, 6 and 8, which led to $p = 14$, 17 and 20 for $n = 200$; $p = 21$, 25 and 30 for $n = 400$; and $p = 29$, 34 and 40 for $n = 800$, respectively.

We carried out 500 simulations for each of the (p, n)-combinations and for each of the two innovation distributions. Figure 1 displays Q-Q plots of standardized empirical likelihood ratio

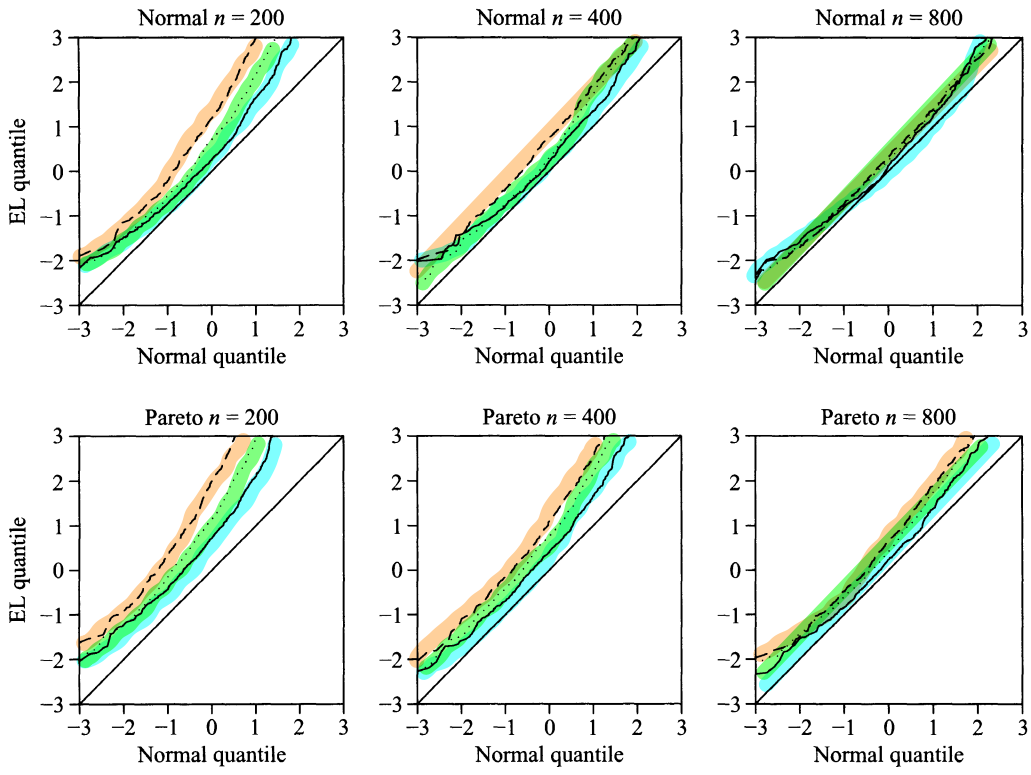

Fig. 1. Normal Q-Q plots with the faster growth rate $p = c_1 n^{0.4}$ for the normal (upper panels) and the Pareto (lower panels) innovations: $c_1 = 3$ (solid line), 4 (dotted lines) and 5 (dashed lines).

statistics for the faster growth rate (i). Those for the slower growth rate (ii) are presented in Fig. 2. As n and p were increased simultaneously, there was a general convergence of the standardized empirical likelihood ratio to $N(0, 1)$. We also observed that the convergence in Fig. 2 for the slower growth rate setting (ii) was faster than that in Fig. 1 for the faster growth rate setting. This is expected as the setting (i) ensured much higher dimensionality. The convergence for the normal innovation was faster than that for the Pareto case when $p = c_1 n^{0.4}$ in Fig. 1. This may be explained by the fact that the Pareto distribution has only finite fourth moments, which corresponds to $k = 1$, whereas the normal innovation has all moments finite. According to Theorems 2 and 3, the growth rate for p depends on the value of k: the larger the k, the higher the rate. For the lower growth rate in setting (ii), Fig. 2 shows that, there was substantial improvement in the convergence in the Q-Q plots as p was increased at the slower rate for both distributions of innovations.

It is observed that the most of the lack-of-fit in the $N(0, 1)$ Q-Q plots in Figs. 1 and 2 appeared at the lower and upper quantiles. This could be attributed to the lack-of-fit between χ^2_p and $N(0, 1)$, as χ^2_p may be viewed as the intermediate convergence of the empirical likelihood ratio.

To verify this, we carried out further simulations by inverting settings (i) and (ii) so that for a given dimension p, three sample sizes were generated according to (iii) $n = (p/c_1)^{1/0.4}$ and (iv) $n = (p/c_2)^{1/0.24}$, with $c_1 = 3$, 4 and 5 and $c_2 = 4$, 5 and 6, respectively. We chose $p = 35$, 45 and 55 for the setting (iii) and $p = 17$, 20 and 25 for the setting (iv). Two figures of χ^2_p-based Q-Q plots for (iii) and (iv), given in the Iowa State University technical report, show that there was a substantial improvement in the overall fit of the Q-Q plots, and that the lack-of-fit in the $N(0, 1)$-based Q-Q plots largely disappeared.